

CSU REPORT
MODELING RESULTS FOR CdS/CdTe SOLAR CELLS

Alan Fahrenbruch, A.L.F. Inc.

March 2000

1. Introduction

There are several general purposes of this modeling including:

- a) Visualizing the carrier transport properties such as fields, potentials, carrier densities, currents, and regions of high recombination and the effects of illumination on transport in CdS/CdTe solar cells.
- b) Evaluating the effects of materials parameters (e.g., acceptor density) and design parameters (e.g., layer thickness) on cell operation.
- c) As a source of ideas of measurements of materials properties and cell parameters.

An article on modeling for the CdS/CdTe cell by Burgelman et al.¹ is recommended.

The following sections include discussions of:

- a) Upgrades of the optical data used in AMPS: the AM1.5G spectrum and the absorption coefficients of CdS and CdTe and a comparison of AMPS and experimental spectral response curves,
- b) Effects of variation of acceptor density and minority carrier lifetime in the CdTe layer on the photovoltaic variables J_{sc} , V_{oc} , ff, and efficiency,
- c) Effects of variation of the thickness of the CdTe layer on the photovoltaic variables, and
- d) Conclusions from the simulations and next steps.

2. Optical data for AMPS

A newer version AMPS-1D² (version 1,0,0,1) was obtained which has the capacity to use more spectral response (SR) data points. This enables better definition of the spectra which is especially important near the CdS band gap edge where experimental data is most affected by cell properties.

New AM1.5G solar spectrum data was input which better matched the ASTM E 892 (100 mW/cm²) standard from NREL. (This must be input point by point and then cloned. It can't be accessed from the "Use AM1.5 Illumination" button in AMPS.) Additional points were added near the band gap edges of CdS and CdTe as well as extending it to shorter wavelengths needed by the thin CdS cells.

¹ M. Burgelman, P. Nollet, and S. Degraeve, Thin Solid Films **361-362**, 527 (00) (special issue on E-MRS Conf., Symposium O: Chalcogenide semiconductors for Photovoltaics).

² Modeling results were obtained using AMPS-1D, version 1,0,0,1, written under the direction of S. Fonash at Pennsylvania State University and supported by the Electric Power Research Institute.

A literature search was done to verify and extend the absorption coefficients (α) of CdS and CdTe as shown in Figs. 1 and 2, along with the data chosen to be used with AMPS. The data from various researchers was generally found to be in two groups: those that were in close agreement with each other (and with Albin's data) and those

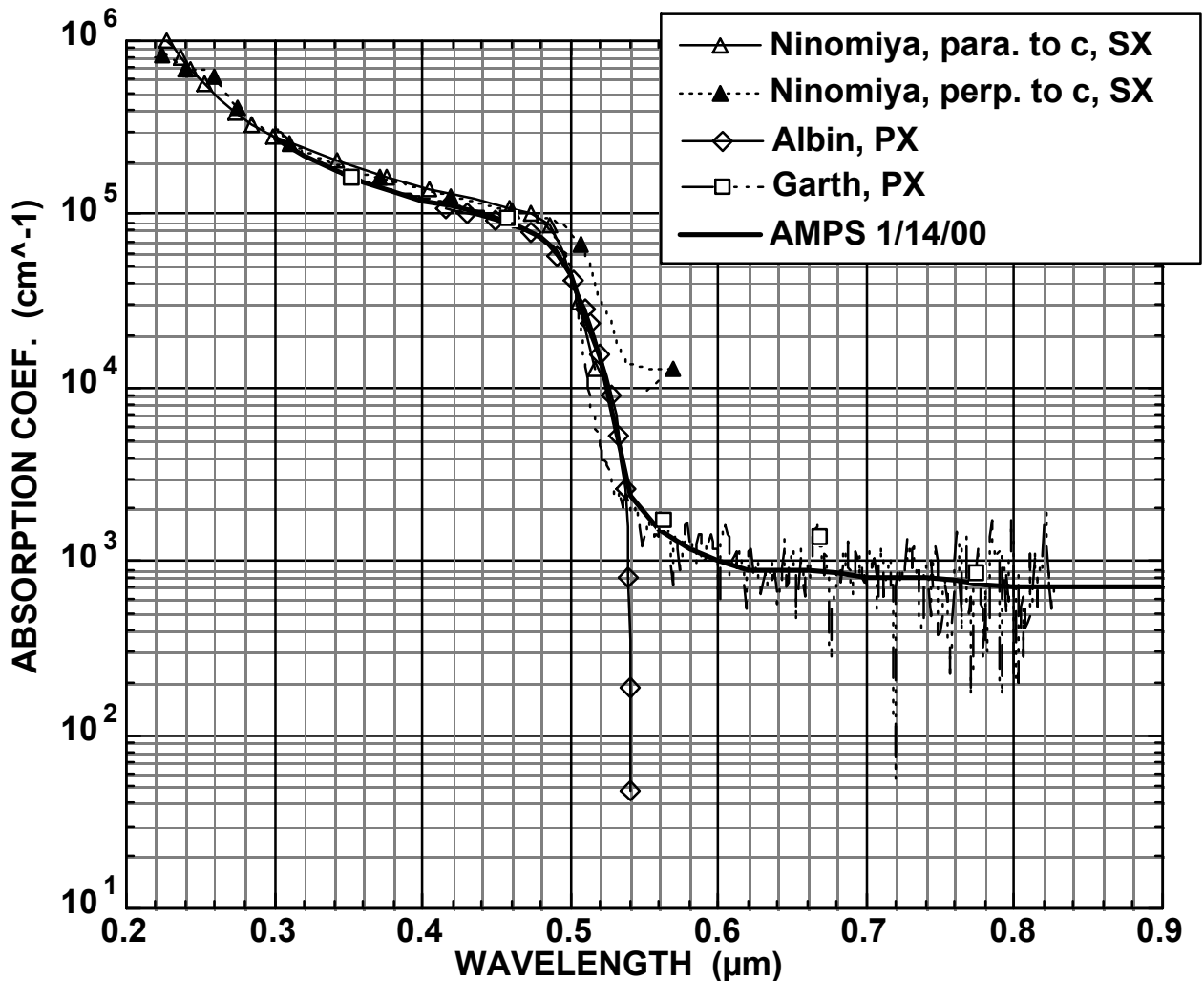


Fig. 1. Absorption coefficient data for CdS. SX data from Ninomiya et al. *J. Appl. Phys.* **78**, 1183 (95), E vector parallel and perpendicular to the c-axis. PX data from D. Albin, NREL, for films from A. Compaan (pulsed laser deposition) and G. Jensen, private communication. (Points shown are on experimental curves but do not correspond to original data points.)

which were clearly outliers. Only the "close agreement" data is shown. Significantly, for both CdS and CdTe, the most consistent data for polycrystalline (PX) thin films was found to lie very close to that of single crystal (SX) material. Long wavelength ($> 0.55 \mu\text{m}$) tail was chosen for AMPS to represent non-useful absorption in the CdS window.

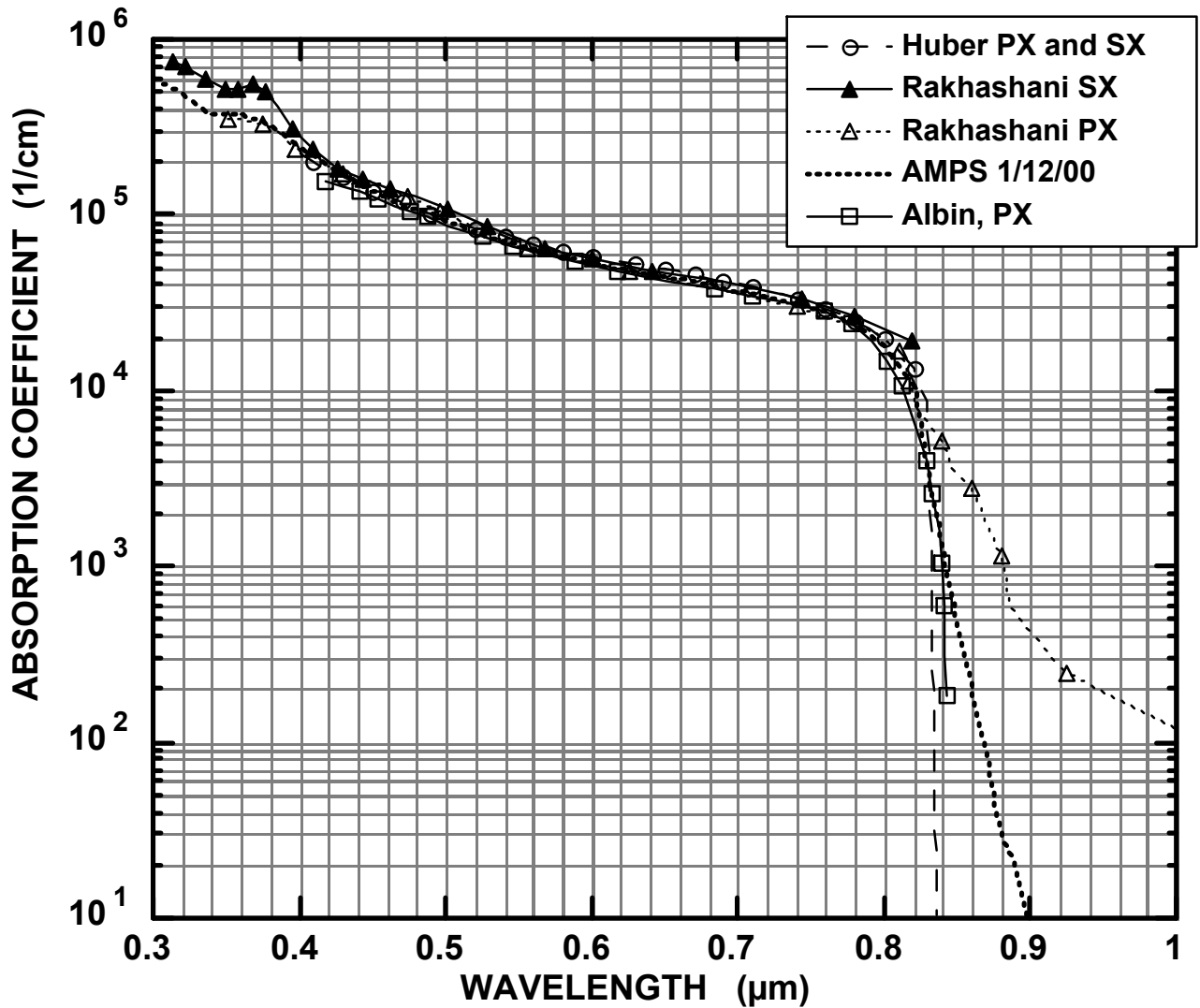


Fig. 2. Absorption coefficient data for CdTe. SX and PX (vacuum evaporated) data from A.E. Rakhashani, J. Appl. Phys. **81**, 7988 (97). Data from W. Huber, PX from a compilation of literature data. PX data from D. Albin, NREL, for films from A. Compaan (pulsed laser deposition). (Points shown are on experimental curves but do not correspond to original data points.)

A comparison of SR data from AMPS and from experiment (Fig. 3) shows close agreement (except for interference effects which are not handled by AMPS). The short wavelength shoulder is strongly affected by the thickness of the CdS layer. The AMPS SR shows a sensitivity to bias light which will be discussed below.

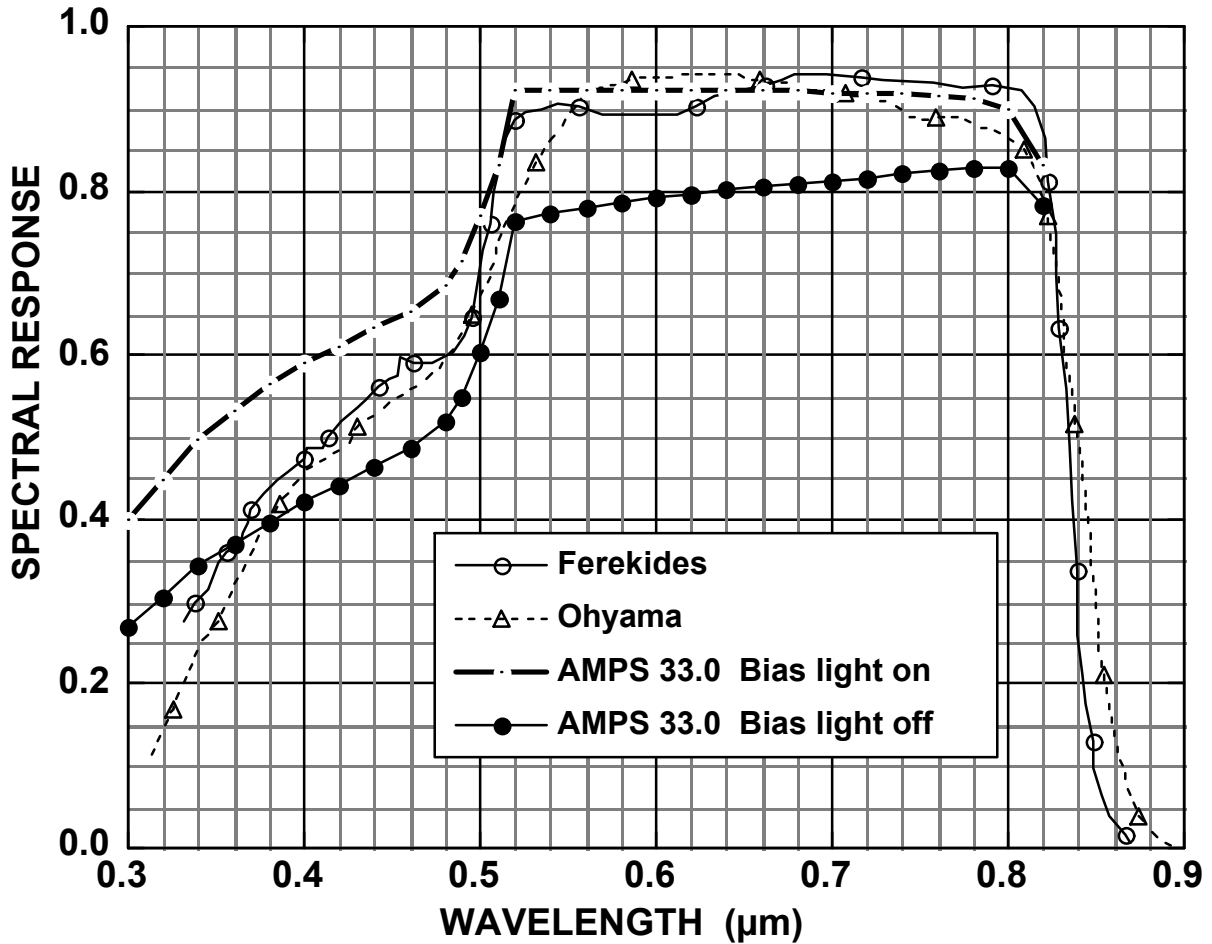


Fig. 3. Comparison of AMPS SR with experimental data. $N_a = 10^{14}$, $\tau = 10^{-9}$, $x_{CdS} = 0.1 \mu m$, $x_{CdTe} = 2 \mu m$. From Ferekides et al. 26th IEEE PV Spec. Conf. ('97) p. 339, Fig. 6, and Ohyama et al. 26th IEEE PV Spec. Conf. (97) p. 343, fig. 4.

3. Influence of Acceptor Density and Minority Carrier Lifetime in the CdTe layer

Choice of Parameter Values

Previous modeling used three sub-layers of CdTe with different acceptor densities (N_a) to replicate N_a profiles obtained from C-V measurements in experimental cells. Since the variations of each of the sub-layers yielded differences of only secondary magnitude, it was decided to simplify the entire CdTe layer to one N_a for this report. The measured range of N_a in real cells is 10^{13} to 10^{15} cm^{-3} , from C-V measurements.³

The thickness of the CdTe was chosen as $2 \mu m$ for these cases (cf., 2 to $8 \mu m$ for most experimental cells), enough to absorb virtually all the solar photons.

³ See, for example, J. Hiltner and J. Sites, NCPV Program Review, AIP Conf. Proc. 462 (1998) p. 170 and D. Rose, D. Rose, First Solar, CdTe Team Meeting, 9/8/98.

A back-contact barrier height $\Phi_{bc} = 0.30$ eV was chosen on the basis of previous modeling⁴ and measurements of contact resistance vs. temperature. Above this value, the back contact barrier begins to substantially affect the ff and the J-V curves above V_{oc} .

A CdS layer thickness of $0.1 \mu\text{m}$, a donor density $N_d = 10^{17} \text{cm}^{-3}$, and a slightly accumulated ohmic contact ($\Phi_{ic} = 0.1$ eV; for $N_d = 10^{17} \text{cm}^{-3}$, $E_{CB} - E_F = 0.135$ eV), and was chosen to de-emphasize the effects of the CdS for these cases.

A summary of AMPS input parameters is given in Table 1.

Table 1. Parameter values.

	Front Contact	n-CdS	p-CdS _x Te _{1-x}	p-CdTe	Back Contact
Reflection	0.07	–	–	–	0.30
Barrier height (eV)	0.1	–	–	–	0.3, var.
Recombination. velocity, electrons (cm/sec)	10^7	–	–	–	10^7
Recombination. velocity, holes (cm/sec)	10^7	–	–	–	10^7
Thickness (μm)	–	0.1	0.1	2, var.	–
Dielectric Coefficient.	–	9.0	9.4	9.4	–
Electron affinity	–	4.50	4.28	4.28	–
Band gap (eV)	–	2.42	1.41	1.50	–
Density of states, CB (cm^{-3})	–	1.8×10^{19}	7.5×10^{17}	7.5×10^{17}	–
Density of states, VB (cm^{-3})	–	2.4×10^{18}	1.8×10^{18}	1.8×10^{18}	–
Carrier density (cm^{-3})	–	10^{17}	10^{14} , var.	10^{14} , var.	–
Electron mobility ($\text{cm}^2/\text{V-sec}$)	–	350	500	500	–
Hole mobility ($\text{cm}^2/\text{V-sec}$)	–	50	60	60	–
Lifetime (sec)	–	10^{-9}	var.	var.	–
Recombination center density N_r (cm^{-3})	–	10^{15}	var.	var.	–
Recombination center energy E_r (eV), wrt. VB	–	1.21	0.75	0.75	–
Recombination cross section σ_n (cm^2)	–	10^{-15}	10^{-12}	10^{-12}	–
Recombination cross section σ_p (cm^2)	–	10^{-12}	10^{-15}	10^{-15}	–

Description of the Recombination Mechanism

Recombination centers play two roles in CdS/CdTe cells: a) as energy levels involved in radiative and non-radiative recombination, and b) to modify the charge density of the layers by acting as deep donors and acceptors when they are empty. Since the occupancy of these levels is determined by recombination traffic, it depends on illumination and bias and thus produces transient influences on the carrier transport (e.g., by deforming the dark, equilibrium band profiles).

AMPS always calculates recombination rates (U) using the Shockley-Read-Hall (SRH)⁵ formalism which requires specification of the recombination center density (N_r), energy

⁴ See, for example, J. Sites, Annual Report (1994), NREL Subcontract XAX-4-14000-01, p. 6 and A.L. Fahrenbruch, NCPV Program Review, AIP Conf. Proc. **462** (1998) p. 48.

level (E_r), and recombination cross sections σ_n and σ_p for each center. The cross sections and N_r enter the SRH equation only in the products $\tau_{no} = 1/N_r v_{th} \sigma_n$ and $\tau_{po} = N_r v_{th} \sigma_p$, where v_{th} is the thermal velocity of the electrons ($\sim 10^7$ cm/sec).⁶ The value N_r affects the charge density and hence the band shape, while σ_n affects only the recombination rate. Thus, for the same values of τ_{no} and τ_{po} , large N_r and small σ values will emphasize the effects of the N_r charge on the band shape, while small N_r and large σ values will minimize the distortion of the bands by N_r charging. Also, the ratio of the cross sections of the centers is important in determining their relative occupancy. For example, a small ratio of σ_n/σ_p will tend to favor a small occupancy of donor-like levels, and their contribution to the space charge will be larger than that for a large σ_n/σ_p ratio.

AMPS has two modes of operation: (a) the so-called Lifetime mode, in which the recombination is characterized by a lifetime $\tau_n = (n - n_0)/U$ which is assumed to be constant, and (b) the unfortunately named Density of States (DOS) mode in which N_r , (E_r), σ_n , and σ_p are used. Although one inputs a lifetime value in the Lifetime mode, the SRH formalism is still used. AMPS assigns a value of N_r and $E_r = E_g/2$ and then calculates σ_n and σ_p that correspond to the given minority carrier lifetime (τ). AMPS chooses a small value of N_r (10^{13} cm⁻³) so as to minimize charging effects due to the change of occupancy of the recombination centers. This works well as long as $N_a \gg 10^{13}$ cm⁻³, but for smaller N_a gives rise to dependences on illumination intensity such as those shown in Fig. 3, where the SR is different with or without bias light. For a true lifetime mode, τ would be assumed to be constant and independent of illumination level, and since the transport equations are linear, the SR should be independent of bias illumination level by assumption (although real cells do show a bias light dependence). Even when using the seemingly more convenient Lifetime mode, the AMPS manual advises a consistency check to make sure the lifetime that AMPS calculates is consistent that entered.⁷

For the DOS cases comparisons a capture ratio of $\sigma_n/\sigma_p = 10^3$ for donor-like centers was used with $\sigma_n = 10^{-12}$ cm² for electrons to a hole occupied donor-like center (+) and $\sigma_p = 10^{-15}$ cm² for holes to an electron occupied donor (neutral).⁸ These values call for N_r values similar in magnitude to N_a which will modify the band shapes between light and dark, supporting the experimental observations of transient behavior.

To summarize, arguments in favor of the DOS mode include:

⁵ See for example, S.M. Sze, "Physics of Semiconductor Devices," 2nd Edition, Wiley Interscience (1981) p. 35.

⁶ τ_{no} is the extremum lifetime for electrons (e.g., when all donor-like centers are filled with holes) and τ_{po} is the extremum lifetime for holes (e.g., when all donor-like centers are filled with electrons).

⁷ See AMPS Manual, p. 33.

⁸ e.g. A.L. Fahrenbruch and R.H. Bube, "Fundamentals of Solar Cells", Academic Press (1983) p. 57. The geometric cross section is $\sim 10^{-15}$ cm². The Coulomb attractive cross section, $\sim 10^{-12}$, is discussed by M. Lax Phys. Rev. **119**, 1502 (60) and Ascarelli and Rodriguez, Phys. Rev. **124**, 1321 (61) and **127**, 167 (62).

- a) the effective lifetime in portions of the cell that have high generation rates can be strongly affected by carrier traffic in the recombination centers under, and thus τ is a function of local carrier densities, whereas N_r , E_r , σ_n and σ_p are not,
- b) SR curves for real cells are affected by bias light, and
- c) in the Lifetime mode, the adjustments that AMPS makes on the recombination parameters are not readily visible.

The most cogent argument in favor of the Lifetime mode is that the lifetime is the most directly observable quantity. Experimental values of N_r , E_r , σ_n , and σ_p are usually obtained more indirectly and they are virtually unknown for PX CdTe. It is clear that when the Lifetime mode is used results should be correlated with "DOS" results whenever possible.

Lifetime data for CdTe are sparse but the value range chosen is generally consistent with values reported from PL⁹ and EBIC measurements on SX material. The V_{oc} and fill factor (ff) values predicted by the model must be consistent with experimental values, and these are strongly dependent on τ (or N_r , E_r , σ_n , and σ_p). Thus values of τ (or N_r , E_r , σ_n , and σ_p) are adjusted by the modeler to obtain the proper V_{oc} and ff.

The data of Section 3 were calculated using the Lifetime mode but some comparisons were done with the DOS mode, particularly at low N_a , to investigate the effects of using DOS with its more significant effects on the space charge.

Simulation Results

Fig. 4 shows band diagrams at zero bias calculated by AMPS for several N_a values. Above $N_a = 10^{16} \text{ cm}^{-3}$ most of the CdTe layer is quasi-neutral and the depletion layers are quite narrow. At 10^{15} cm^{-3} the depletion layers fill most of the CdTe and for $3 \times 10^{13} \text{ cm}^{-3}$ and below the electric field is large and constant throughout the CdTe, giving essentially an n/i/p junction. Fig. 5 shows the bands at the maximum power voltage (V_{max}) for $\tau = 10^{-9}$ sec. Even at this early stage of simulation the strong dependence of cell voltage on N_a is apparent.

⁹ E.g., W. Song et al., NCPV Program Review, AIP Conf. Proc. **462** (1998) p. 194.

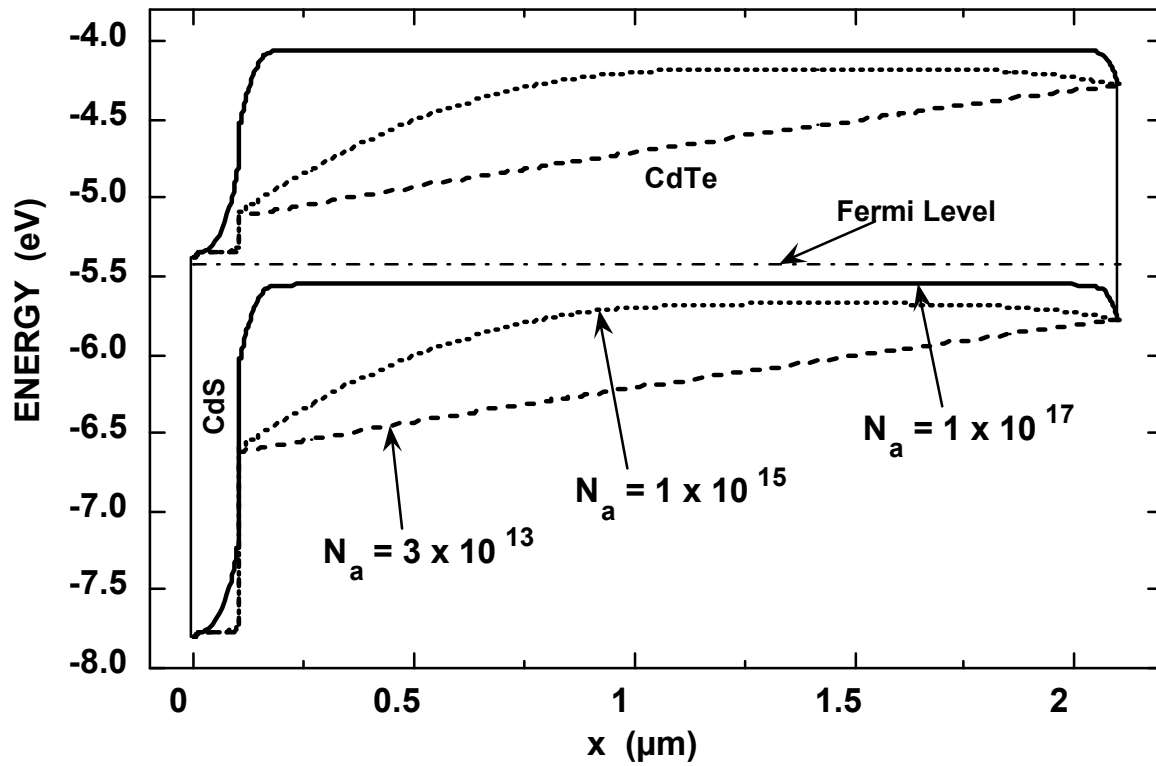


Fig. 4. Simulated band diagrams for zero bias **with light off**. $\phi_{bc} = 0.3$ eV.

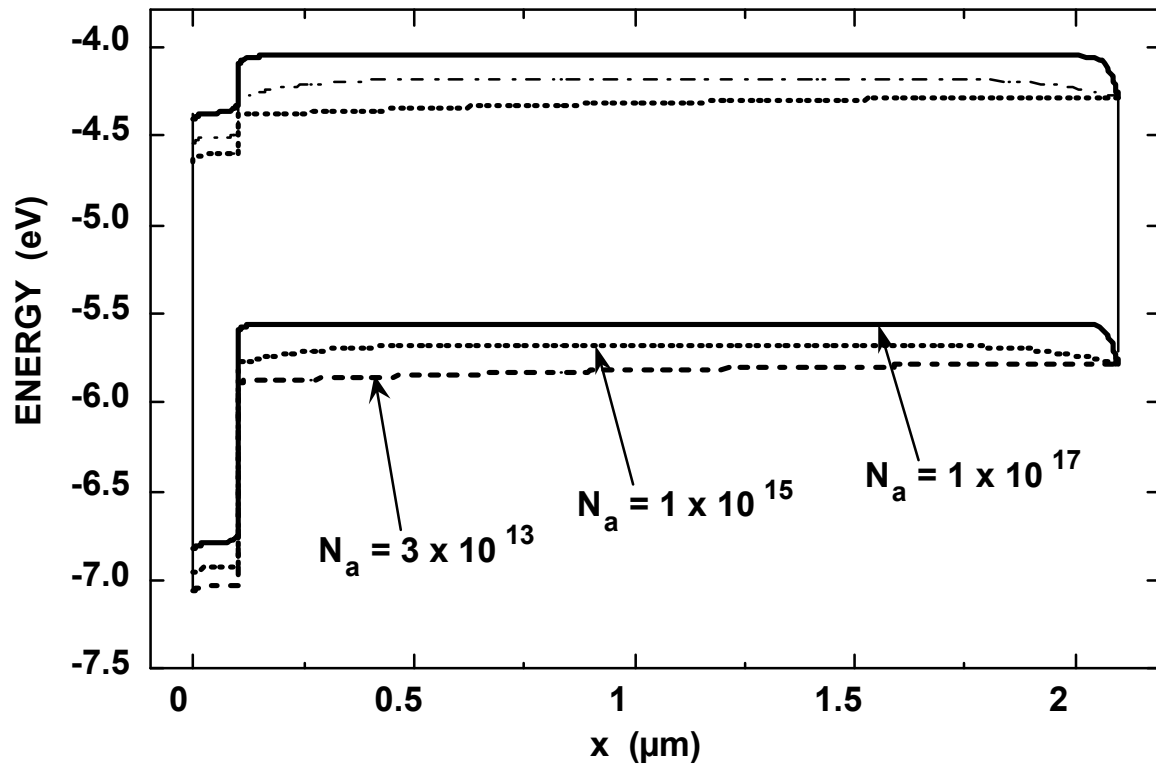


Fig. 4. Simulated band diagrams at the maximum power point, for $\tau = 10^{-9}$ sec.

In Fig. 6 are plots of the generation (gain) and total recombination (loss) vs. distance at V_{\max} . For $N_a = 10^{17} \text{ cm}^{-3}$ a substantial part of the generation is in the field-free quasineutral region and the carriers diffuse through it readily and recombine in the bulk. For $N_a = 10^{15} \text{ cm}^{-3}$, many of the photogenerated electrons face a region of strong reverse field and recombination is highly peaked in this region. For $N_a = 3 \times 10^{13} \text{ cm}^{-3}$ the electric field is lower and relatively constant so the recombination reflects the generation profile.

The variation of J_{sc} , V_{oc} , ff , and efficiency (Eff) is shown in Fig. 7.

Lets focus on J_{sc} first. From Figs. 4 and 5 we saw that the electric field (\mathcal{E}) in the photogeneration region is strongly dependent on N_a . In the presence of \mathcal{E} the effective lifetime τ_{eff} is related to the zero-field lifetime τ_0 by $\tau_{\text{eff}} \sim \tau_0(1 \pm \mathcal{E}/\mathcal{E}_c)^2$, where $\mathcal{E}_c = (kT/\mu\tau)^{0.5}$ and the + is for diffusion along the field and the - is for diffusion against the field.¹⁰ For fairly large values of τ_0 , J_{sc} is asymptotic to its maximum value and variations in τ_{eff} (electric-field-aided collection) have a rather small effect on J_{sc} . For smaller values of τ_0 , field-aided collection plays a much stronger role. In the region of major generation, the field is the highest for $N_a \blacktriangleright 2 \times 10^{15} \text{ cm}^{-3}$, and J_{sc} shows a maximum there.

The V_{oc} decreases rather strongly for decreasing N_a because the potential barrier faced by electrons diffusing across the junction to the right (the bucking current) collapses for smaller N_a . This will be explored more in the next section. At V_{\max} , a significant portion of the recombination loss occurs at the back contact as shown in Table 2.

Table 2. Back surface contact recombination loss.

$N_a \text{ (cm}^{-3}\text{)}$	Back-contact recombination loss ¹¹ (J_{bc}) (mA/cm ²)	J_{sc} (mA/cm ²)	J_{\max} (mA/cm ²)	Relative back-contact to bulk loss, $J_{bc}/(J_{sc} - J_{\max})$ (%)
10^{13}	0.4	- 22.7	- 18.8	10
10^{15}	1.4	- 23.1	- 20.4	52
10^{17}	2.0	- 21.6	- 19.4	91

The ff is given by $ff \blacktriangleright ff_0(1 - J_{sc}R_s/V_{oc})$ for small values of series resistance (R_s), where ff_0 is the inherent ff for $R_s = 0$. Since ff_0 is generally determined by same variables as V_{oc} , the variations in ff_0 with N_a are similar to those for V_{oc} . Because AMPS doesn't account for R_s contributions external to the junction (grids, bus bars, TCOs, etc.) the value of ff_0 must be targeted slightly above the ff values for experimental cells.

¹⁰ e.g. A.L. Fahrenbruch and R.H. Bube, "Fundamentals of Solar Cells", Academic Press (1983) p. 83.

¹¹ Obtained from the plots of electron and hole current vs. distance at V_{oc} .

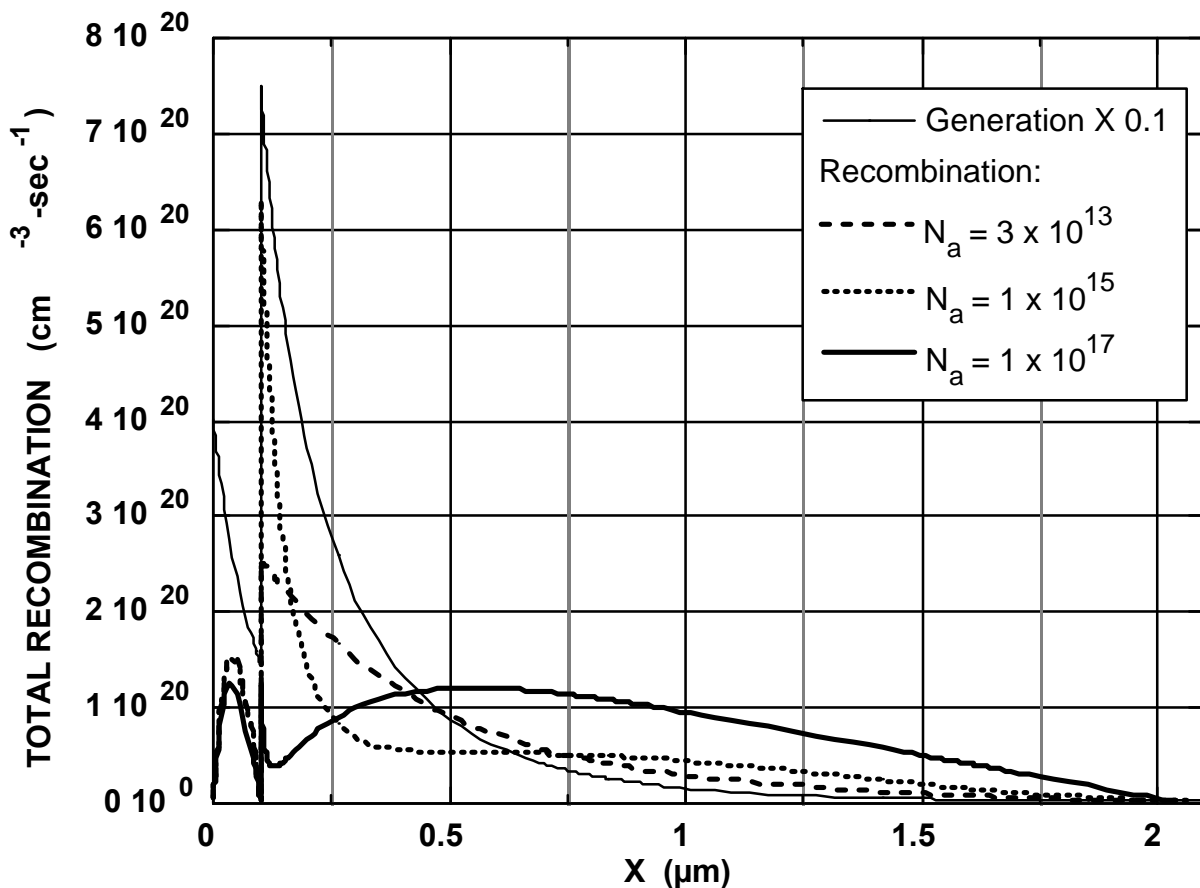


Fig. 6. Generation and total recombination rate vs. distance at the maximum power point, for $\tau = 10^{-9}$ sec.

Target Values

Beyond being consistent with measurable materials properties (α , front and back surface optical reflection, N_d , N_a , etc.) and physical configuration (layer thicknesses, etc.), the most important requirement for a good model is to be able to duplicate the basic PV variables. For simulations of a general nature, the PV variables of the record CdS/CdTe cell of Ferekides et al.¹² were adapted. For later simulations of specific cells, their particular properties will be targets.

The simulated value of J_{sc} must be in a range consistent with the target PV variables, but it can be "fine tuned" by varying the CdS thickness (x_{CdS}), recombination in the CdS, and the reflection coefficients at the front and back of the cell, which are known approximately. In addition its specific value is not strongly interconnected with the values of V_{oc} and ff . Thus it was decided to focus on V_{oc} and ff and target J_{sc} separately.

On the other hand, V_{oc} and ff are strongly coupled, and for the model presented here (either in Lifetime or DOS mode), bringing V_{oc} down to target values (e.g., by decreasing τ) always resulted in a ff_0 that was too small (Fig. 7). Although not exhaustive, other

¹² C. Ferekides et al., Proc. 23rd IEEE PV Spec. Conf. (1993) p. 389. $J_{sc} = 25$ mA/cm², $V_{oc} = 0.85$ V, $ff = 0.75$, and $Eff = 15.8\%$.

simulations using various N_a profiles and interfacial recombination layers did not promise simultaneous targeting of V_{oc} and ff.¹³; ff_0 was always too small if V_{oc} was targeted.

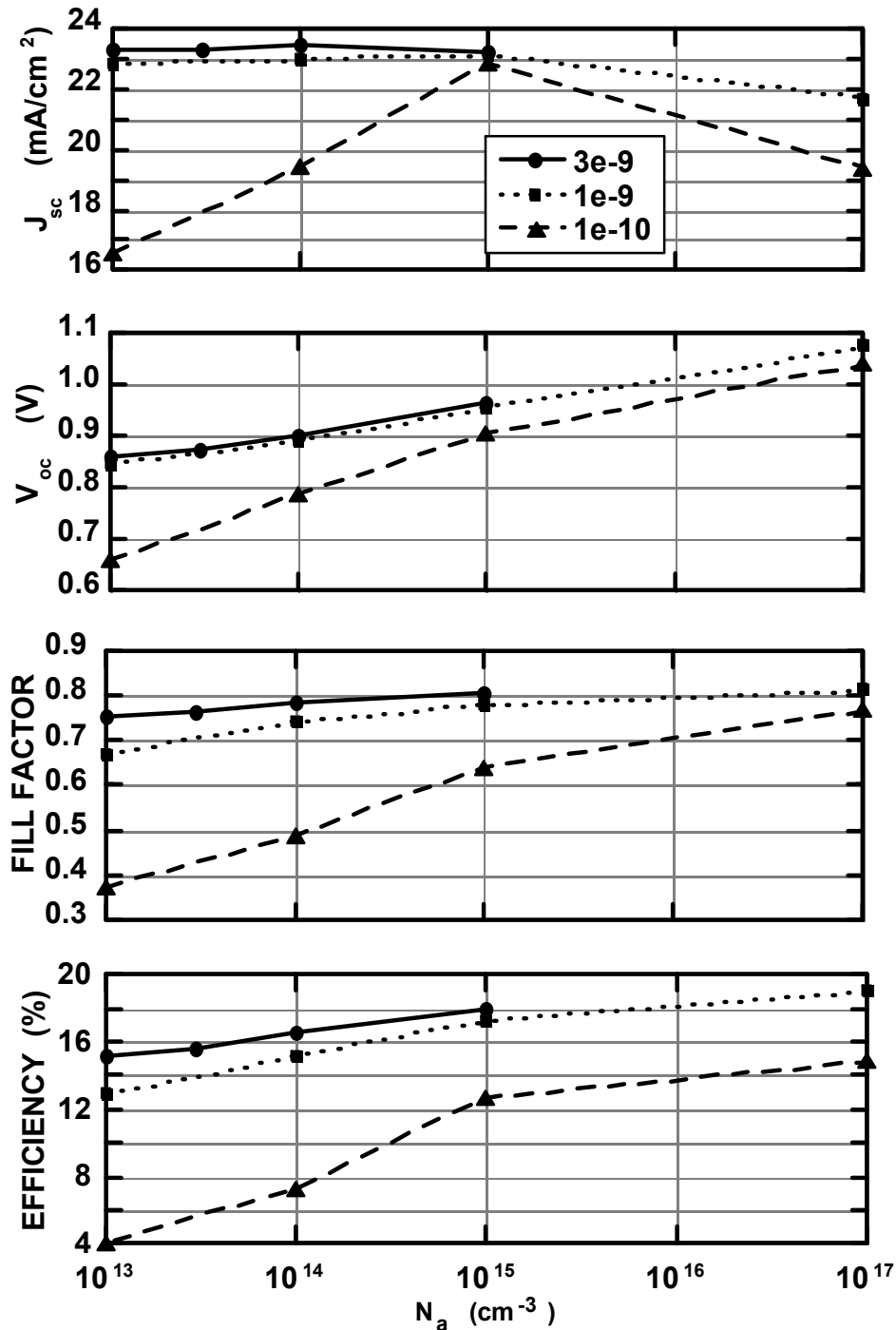


Fig. 7. J_{sc} , V_{oc} , ff, and Eff vs. N_a and lifetime. $\Phi_{bc} = 0.3$ eV. CdS reflection = 0.07. $X_{CdS} = 0.1$ μm .

¹³ It was necessary to invoke a CdSTe layer to simultaneously target V_{oc} and ff. This is discussed in ITN Annual Report 2/2000.

4. Variation of CdTe layer thickness

The variation of CdTe layer thickness yielded a surprising number of insights. For these cases, $N_a = 10^{14} \text{ cm}^{-3}$ was used, with two extreme cases: $\phi_{bc} = 0.0$ and 0.5 eV . Using $\phi_{bc} = 0.0 \text{ eV}$ gives an accumulation region at the back contact which acts as a both an ohmic contact and a minority carrier mirror, a most desirable condition but most likely never achieved (or achievable) in real cells. On the other hand, the results for $\phi_{bc} = 0.5 \text{ eV}$ show the typical anomalies which occur as a result of environmental stressing of experimental cells. The remaining quantities are as in Table 1.

The band diagrams for these cases (LT mode) are shown in Fig. 8 at zero bias and the corresponding PV variables are shown in Fig. 9.

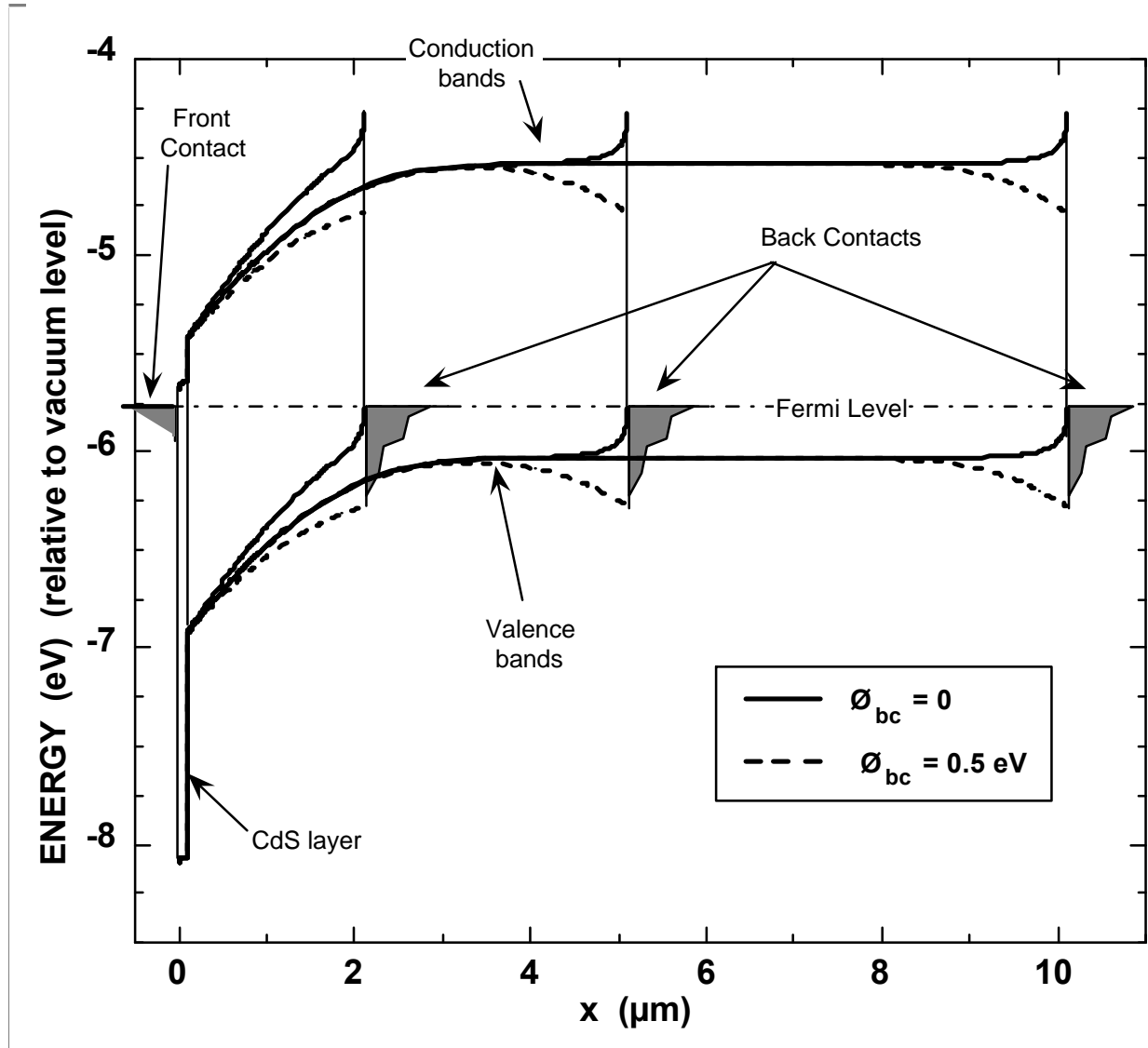


Fig. 8. Band diagrams for the CdTe thickness variation cases for $\phi_{bc} = 0$ and 0.5 eV (LT mode, $V = 0$, dark).

J_{sc} is relatively insensitive to ϕ_{bc} . The dropoff in J_{sc} at smaller thicknesses is as expected due to lessening of the absorption volume.

For $\phi_{bc} = 0$, the ff follows the variation of V_{oc} , as expected.

However, for $\Phi_{bc} = 0.5$ eV, the ff does not follow the variation of V_{oc} , but increases for thinner CdTe layers because the collapse of the barrier for $x_{CdTe} \approx 2 \mu m$ changes the character of the back contact, making it ohmic for photogenerated holes traveling to the right.

Again, simultaneous targeting of V_{oc} and ff is not possible, with ff_0 being too low for reasonable values of the parameters.

Since the depletion layer widths depend on N_a , the observed changes take place for thicker (thinner) CdTe layers for lower (higher) N_a values.

The J-V characteristics for a CdTe thickness of $0.5 \mu m$ in Fig. 10 shows almost identical J_{sc} and similar ff values for both $\Phi_{bc} = 0$ and 0.5 eV, but V_{oc} is different by almost 0.4 eV. The back contact barrier with $\Phi_{bc} = 0.5$ eV is not a barrier to photo-generated holes, but just decreases the effective junction barrier of the cell. The light and dark curves do not cross for $\Phi_{bc} = 0$ and cross only at higher currents (~ 200 mA/cm²) for $\Phi_{bc} = 0.5$ eV.

For $\Phi_{bc} = 0$, V_{oc} becomes larger for thinner CdTe because the recombination volume becomes smaller and the accumulation layer at the back contact reduces the surface recombination there to very small values.

For $\Phi_{bc} = 0.5$ eV, V_{oc} is strongly reduced for thinner cells because the barrier to transport of electrons to the right (bucking current) collapses between $2 \mu m$ and $5 \mu m$. In these cases the reverse field at the back is lessened or nonexistent and there is no barrier to photogenerated holes, which in turn strongly increases recombination loss at the back contact. For $\Phi_{bc} = 0.5$ eV, the loss current through bulk recombination in the $2 \mu m$ CdTe case is smaller (by a factor of 2) than that of the $5 \mu m$ CdTe (smaller recombination volume). However, the surface recombination loss at the back contact¹⁹ is larger by a factor of 7 for the $2 \mu m$ cells. Thus the reverse field at the back essentially turns the back surface recombination on or off.

For $\Phi_{bc} = 0$, Fig. 11, there is little difference between the light and dark JV curves for 2 and $5 \mu m$, and the light and dark curves do not cross.

For $\Phi_{bc} = 0.5$ eV, Fig. 11, and $x_{CdTe} = 2 \mu m$, there is strong crossover of light and dark JV curves but no rollover. Increasing the thickness to $5 \mu m$ causes a strong rollover of the JV curves for $V > V_{oc}$ because of the development of a barrier to photogenerated holes at the back contact (Fig. 8).

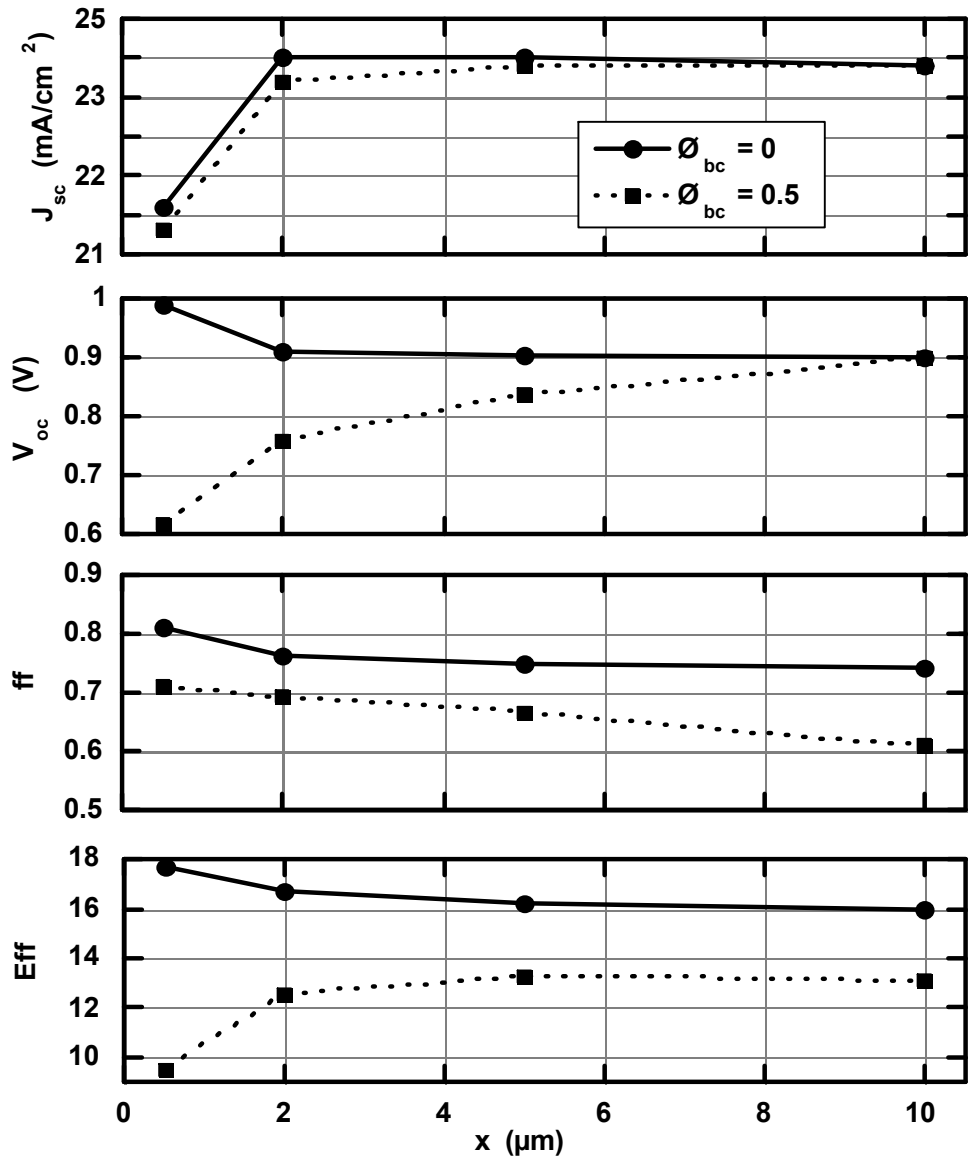


Fig. 9. PV variables for the CdTe thickness variation cases ($N_a = 10^{14}$, $\tau = 10^{-9}$ sec).

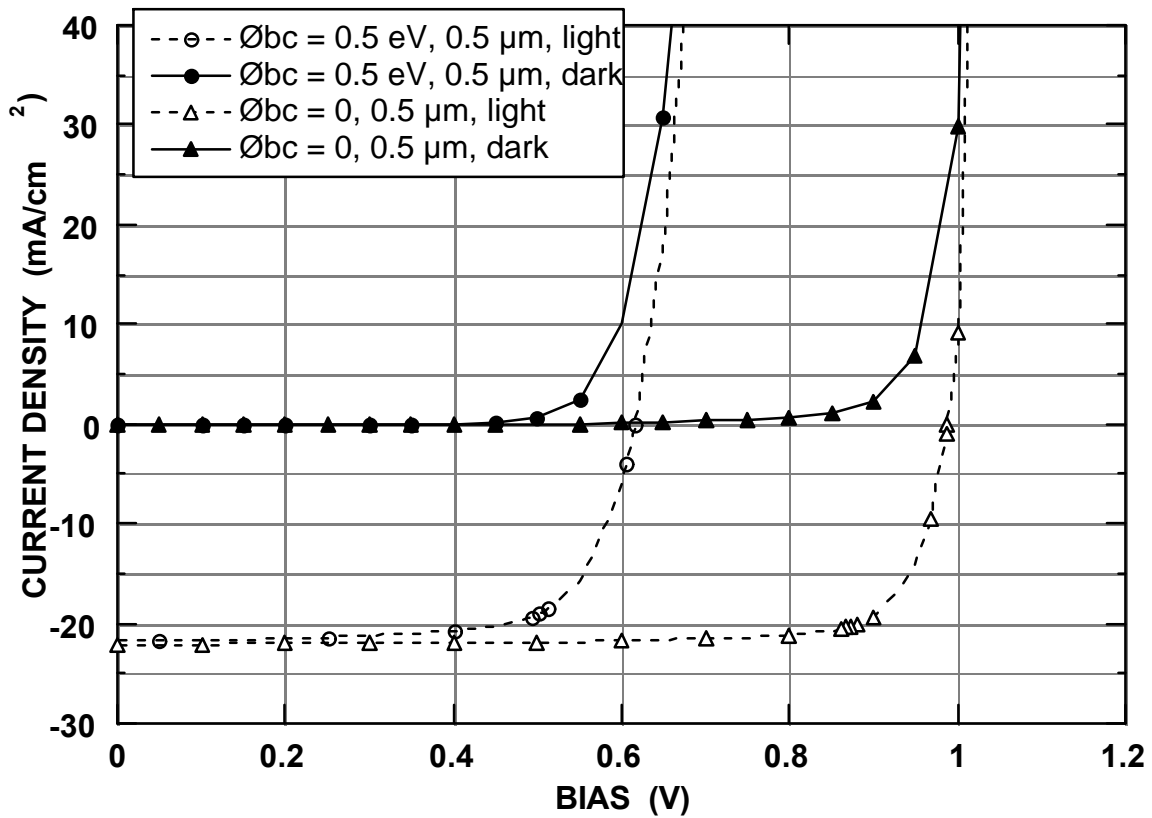


Fig. 10. J-V curves for the CdTe thickness = 0.5 μm. ($\tau = 10^{-9}$ sec).

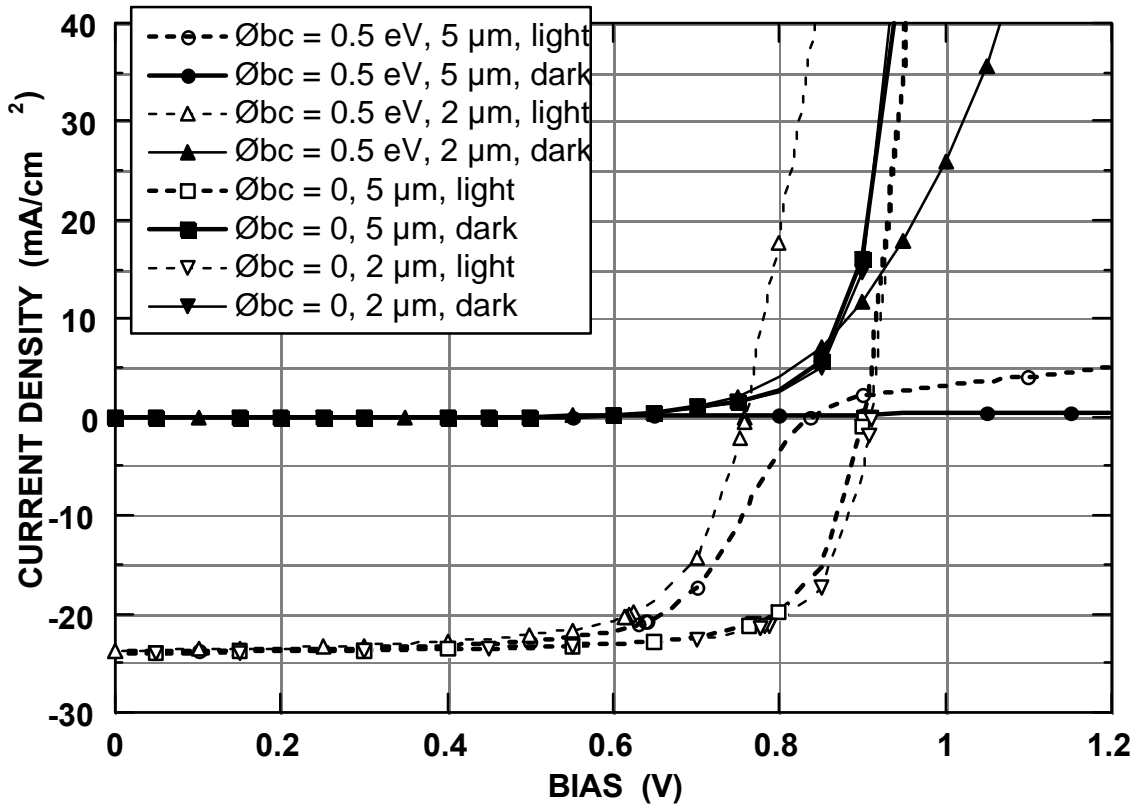


Fig. 11. J-V curves for the CdTe thickness = 0.5 μm. ($\tau = 10^{-9}$ sec).

These simulated J-V curves always show a bias dependent light generated current [$J_L(V)$] which lowers V_{oc} and ff from their ideal values. This is the breach of superposition of dark and light J-V curves which is so characteristic of all experimental CdS/CdTe cells. If the lifetime is increased to unreasonably high values for CdTe (10^{-5} sec), superposition is regained.

5. Conclusions and Next Steps

- The AMPS data for the AM1.5G spectrum and the CdS and CdTe absorption coefficients were verified and extended.
- For variation of the PV variables with N_a and τ this modeling showed that:
 - Greater N_a gives higher efficiency.
 - V_{oc} decreases strongly for decreasing N_a because the potential barrier faced by electrons diffusing across the junction to the right (the bucking current) collapses for smaller N_a .
 - Given the high J_{sc} values shown by most experimental cells, this modeling suggests that the effective carrier lifetime is already quite large and that further increases will only marginally increase V_{oc} , ff , and efficiency; the largest potential for improvement is in increasing N_a .
 - For smaller CdTe layer thicknesses ($\square 2 \mu\text{m}$, at $N_a = 10^{15} \text{ cm}^{-3}$), back contact surface recombination is a large part of the loss current at V_{max} .
 - Although the target PV variables can be closely approached for low N_a , the ff was always too small if V_{oc} was adjusted to the target value (e.g., by changing τ).
 - For smaller values of τ , electric field-aided collection plays a strong role in determining J_{sc} .
- Variation of the PV variables with CdTe layer thickness demonstrates the strong influence of back contact barrier height, giving rise to the anomalies (V_{oc} shift, cross-over, and roll-over) that are commonly seen, particularly for stressed devices:
 - For a CdTe thickness of $0.5 \mu\text{m}$, J_{sc} and ff values are very similar for both $\phi_{bc} = 0$ and 0.5 eV , but V_{oc} shifts by almost 0.4 eV . The back contact with $\phi_{bc} = 0.5 \text{ eV}$ is not a barrier to photo-generated holes in this case, but just decreases the effective junction barrier of the cell.
 - For $\phi_{bc} = 0$ there is little difference between the light and dark JV curves for 2 and $5 \mu\text{m}$, and the light and dark curves do not cross.
 - For $\phi_{bc} = 0.5 \text{ eV}$, as the CdTe thickness is reduced from 5 to $2 \mu\text{m}$, V_{oc} is significantly reduced because the barrier to transport of electrons to the right (bucking current) collapses. In addition, the barrier to photogenerated holes to the back contact disappears, strongly increasing recombination loss at the back contact.
 - For $\phi_{bc} = 0.5 \text{ eV}$ and $x_{CdTe} = 2 \mu\text{m}$, there is strong cross-over of light and dark JV curves but no rollover. For $x_{CdTe} = 5 \mu\text{m}$, there is a strong roll-over of the JV curves

for $V > V_{oc}$ because of the development of the barrier to photogenerated holes at the back contact.

Given the addition of a CdSTe alloy layer (discussed elsewhere²⁰), these rather simple AMPS models can duplicate the generic PV variable targets almost exactly using a combination of experimental data and physically reasonable parameters. Other areas of agreement are summarized in Table 2.

DOS mode comparisons to these Lifetime mode results (which use more realistic values for N_r and cross sections) give similar overall qualitative results but with some added complexities. One of the major steps in further refining these simulations is the quantification of bulk and surface recombination parameters. This requires investigation of the extent of transient effects and their time-temperature dependences. Part of this exists in the literature, but some additional experimental work will probably be needed. In addition, incorporation of information on the recombination centers themselves (E_r , N_r , τ , etc.) in CdTe is important. AMPS can not model transient behavior, but it can model end states such as SR and $N_a(x)$ profiles (from capacitance-voltage data) with and without bias light. The time-temperature dependences for the change between end states gives information about the depth of the recombination centers (E_r).

Other information required for more realistic simulations includes the interface recombination velocities S_{bc} , S_{fc} , $S_{CdS/CdTe}$, and $S_{TCO/CdS}$ (each for electrons and holes) and electron affinity (or band discontinuity values) for TCO and the front contact (e.g., χ_{E_c} , χ_{E_v} values for fc/CdS , fc/TCO , CdS/TCO , $TCO/CdTe$, $CdS/CdTe$).

The next steps to be taken are:

- simulation of particular cells (those with the most experimental data), hopefully following them through stressing,
- determination of the effects of front-contact barrier height, and
- refinement of back contact barrier effects after stressing.

Table 2. Areas of comparison of simulation with experimental cells.

TOPIC	PRINCIPAL DETERMINERS	COMMENT
Spectral response (SR)	Band gaps, x_{CdS} , and to a lesser extent, τ and N_a	Excellent quantitative agreement (except for interference effects)
Bias light dependence of SR	Charge in deep states ($N_r, \sigma_n/\sigma_p$)	Qualitative agreement
Bias dependence of J_L	N_a profile, τ	Good qualitative agreement
J_{sc}	SR, reflection, x_{CdS} in asymptotic range (x_{CdTe}, τ, N_a in lower range)	Excellent quantitative agreement in asymptotic range
V_{oc}	N_a, τ, x_{CdTe} (Φ_{bc} for small x_{CdTe})	Fair quantitative agreement using low N_a
ff	N_a, τ, x_{CdTe} (Φ_{bc} for small x_{CdTe})	Same
V_{oc}, ff simultaneously	As above	Excellent quantitative agreement with CdS layer present
TC of V_{oc}	Main barrier, E_r	To be investigated
Cross-over of light and dark J-V w. stress	$\Phi_{bc}, (N_a?)$	Qualitative agreement obtained by varying Φ_{bc} in previous report. Revisit: can changes in N_a alone explain cross-over (with Φ_{bc} const.)?
Roll-over of dark J-V above V_{oc} with stress	$\Phi_{bc}, (N_a?)$	Qualitative agreement obtained by varying Φ_{bc} in previous report. Revisit: can changes in N_a alone explain roll-over (with Φ_{bc} const.)?
V_{oc} shift with stress	$\Phi_{bc}, x_{CdTe},$ and N_a	Further investigation needed
Transient behavior of SR and J-V	Charge in deep states ($N_r, \sigma_n/\sigma_p$), bias light history	Further investigation needed
Capacitance-voltage results	N_a profile, bias light history	Qualitative agreement obtained with SCAPS ¹⁴ by Burgelman et al.- must be correlated with AMPS results.

¹⁴ SCAPS 1D is a simulation program which handles ac analysis, developed by M. Burgelman et al. at the University of Ghent. It is free to Universities and runs on PC's.